(Received 26 April 2026, Accepted 21 May 2026, Scheduled 30 May 2026)

A Miniaturised Māra Cross-Inspired Fractal Microstrip Sensor for Edible Oil Sensing

Ahmed A. Al-Mudhafar[1, *] and Sarah J. Ghazi[2]

[1] *Department of Communication Technologies Engineering, Engineering Technical College Al-Furat Al-Awsat Technical University, Najaf 31001, Iraq*
[2] *Department of Food Sciences, College of Agriculture, University of Kufa, Iraq*

ABSTRACT: This work introduces an innovative fractal microstrip sensor, shaped like a Māra cross enclosed within a square, designed and fabricated on a Rogers RT5880 substrate for high-precision detection and characterization of edible oils. The proposed resonant shape enhances electric-field concentration and improves the interaction between the material under test and the electromagnetic field, resulting in improved sensitivity and resonant response. The sensor operates at a frequency of approximately 4 GHz within the S-band, with an area of $50 \times 50\,\text{mm}^2$, making it suitable for portable and low-cost applications. The results demonstrated clear frequency shifts for various oil types, including coconut oil, olive oil, sunflower oil, and sesame oil. A mathematical model was also developed to extract the complex electrical permittivity with a high coefficient of determination of 0.99, showing excellent agreement between the experimental and theoretical results. The fractal sensor exhibits a remarkable normalized sensitivity of 0.86% and 3.56% per unit dielectric variation and error of 0.03% and 0.13%, with frequency shifts of 163 MHz and 103 MHz for water and ethanol detection, respectively. Maximum sensitivities reached 15.23% for olive oil and 11.32% for sunflower oil, surpassing many previously published studies.

1. INTRODUCTION

Resonator-based sensors are a modern technology that has garnered significant attention in the field of liquid analysis due to their high accuracy and exceptional sensitivity in detecting physical and chemical changes. Their use is particularly prominent in sensing vegetable oils, given the importance of these oils in the food, pharmaceutical, and cosmetic industries, and the increasing need to ensure their quality and detect adulteration or spoilage resulting from storage or heat exposure [1–3]. Therefore, resonators have become an effective tool for developing rapid, nondestructive measurement systems that enable the efficient evaluation of vegetable oil properties [4–7].

The knowledge of electrical permittivity is important for designing various microwave and radio-frequency circuits and antennas. It is equally important in various industries, such as food quality control, biosensing, and detection of buried objects [2, 5, 8].

Electrical permittivity is an important parameter that provides useful information about the composition of materials and the amount of moisture present in them. As the electrical properties of materials change with various parameters, such as the amount of moisture, the knowledge of electrical permittivity is useful in various applications, such as quality control [6, 8, 11, 12].

In recent years, there has been increasing interest in using resonators and antennas as nondestructive and precise sensors for determining the electrical permittivity of liquids, particularly vegetable oils, due to their significant importance in the food and pharmaceutical industries and quality control [4–6].

These techniques rely on the principle of interaction between the electromagnetic field propagating around the resonator or antenna and the sample being measured. A change in the dielectric properties of the oil leads to a shift in the resonant frequency or a change in the propagation coefficients and dispersion parameters, such as S_{11} and S_{21} [13–15].

Various types of resonators, such as split-ring resonators, microstrip resonators, and planar antennas, have demonstrated high efficiency in sensing minute changes in permittivity and loss coefficient [5–7, 9].

The use of resonators and microwave antennas offers several advantages, including simplicity, low cost, rapid measurement, and compatibility with smart devices. These methods also enable the development of mathematical models that link the resonant frequency and complex electrical permittivity of vegetable oils, contributing to oil differentiation, adulteration detection, and accurate and reliable monitoring of changes in their physical properties [8–10, 16, 17].

Different structures of microwave resonators have been suggested in recent studies for enhancing the accuracy of measurements in permittivity sensing. The symmetric bar chart-type resonator had a sensitivity equal to 2.2% [18], while the contactless resonator sensor exhibited accurate measurement of dielectric characteristics of aqueous solutions, showing a sensitivity equal to 4% [19]. In addition, the planar U-shaped resonator with coupled lines and split-ring resonators was introduced to increase the electric field interaction with liquid samples, resulting in an increase in sensitivity of approximately 45% [20].

* Corresponding author: Ahmed A. Al-Mudhafar (ahmedadnan@atu.edu.iq).

However, there are problems in the improvement of sensitivity, size reduction, and magnetic field focusing in previous resonators.

The proposed sensor is a planar microwave sensor based on fractal microstrip technology and employs a Māra cross-shaped resonant structure as its main sensing element. The sensor is fabricated on a dielectric substrate with a conductive microstrip pattern etched on the top surface and a continuous ground plane on the bottom layer of the substrate. The cross geometry consists of four plus signs (+) arranged around a central cross junction, ensuring geometric symmetry and a uniform electromagnetic field distribution. The sensor was tailored for sensing edible oil, where different oil types induced noticeable shifts in the resonant frequency. The experimental results confirmed that the proposed sensor achieved enhanced sensitivity compared to that reported in the literature.

2. DESIGN AND MANUFACTURING

The suggested sensor is a planar microwave sensor utilizing fractal microstrip technique and uses a Māra cross resonator structure as its primary sensing device, as shown in Fig. 1. The proposed sensor was designed and fabricated on a dielectric substrate using an RT/duroid 5880 laminate material. The dielectric substrate has a thickness of 1.57 mm, relative permittivity of 2.20 ± 0.02, and loss tangent of 0.0009. The copper thickness was 35 µm, with a conductivity of 5.7×10^7 S/m. The microstrip fractal pattern is etched on the top copper surface, and a continuous ground plane is on the bottom layer. The Māra cross geometry consists of four plus signs (+) arranged around a central cross (+) junction and surrounded by a square frame, which ensures geometric symmetry and uniform electromagnetic field distribution.

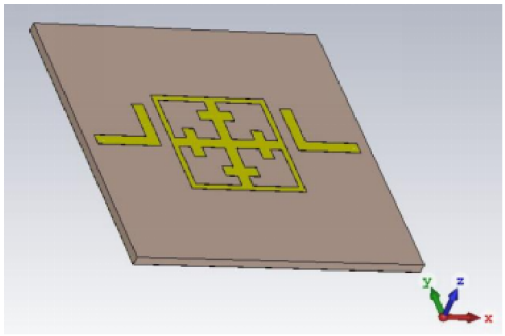

FIGURE 1. A 3D view of the microstrip sensor design structure based on fractal technology.

Figure 2 illustrates the evolution of a rectangular microstrip patch resonator toward a fractal-based geometry, presented in five stages labelled (a)–(e). All configurations were implemented on the same dielectric substrate and shared identical 50 Ω coupling feed lines and ground-plane conditions to ensure a fair electromagnetic comparison using the Computer Simulation Technology (CST) Studio Suite simulation program. Fig. 3 shows the simulated results of insertion loss (S_{21} [dB]) vs. frequency (Freq. [GHz]).

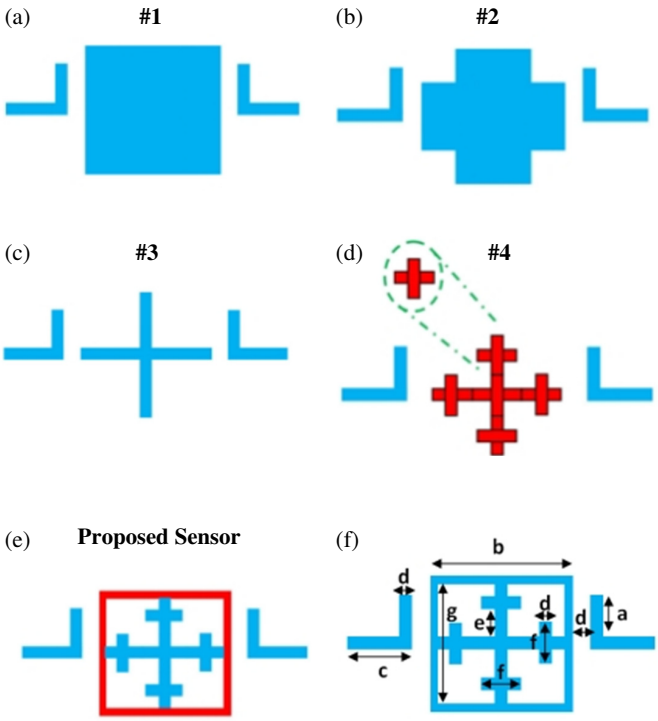

FIGURE 2. Parameter study for the five stages labelled (a) to (e) and (f) optimal sensor's dimensions.

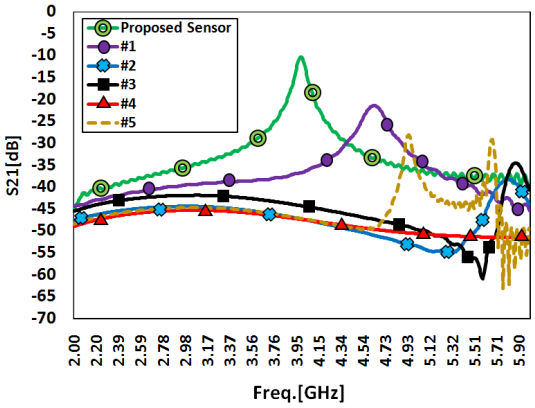

FIGURE 3. Resonator performance in terms of S_{21} parameter for the five cases.

Figure 2(a) shows a conventional rectangular microstrip patch resonator, which serves as the reference design. This structure, with dimensions 20×20 mm^2, supports a fundamental resonant mode determined primarily by the patch dimensions and substrate properties. The resonator exhibited a single dominant resonance at 4.63 GHz with an insertion loss of $S_{21} = -21.5$ dB at the operating frequency.

Figure 2(b) shows a central cross-shaped metallic patch symmetrically extended in both the horizontal and vertical directions. This configuration yields $S_{21} = -38.33$ dB at 5.8 GHz.

Figure 2(c) depicts a decoupled cross-shaped design, consisting of orthogonal horizontal and vertical microstrip lines with a width of 2 mm intersecting at the center, along with other lateral stubs. This design facilitates bidirectional current flow and helps achieve a symmetrical field distribution along both axes.

The separated lines add more capacitive and inductive components, allowing for better control of the resonant frequency and impedance-matching properties. The design shows S_{21} of -37.52 dB at 5.87 GHz.

Figure 2(d) presents a higher-order fractal iteration, where four smaller cross elements, similar to the + sign, are symmetrically attached to the corners of the central cross patch. This modification increases the effective electrical length of the radiator without significantly enlarging its physical footprint. The introduced discontinuities increase the current path complexity and electromagnetic coupling, leading to resonance shifting and potential bandwidth enhancement. The corresponding insertion loss for this configuration is $S_{21} = -45.25$ dB.

Figure 2(e) shows the final proposed sensor, in which an additional square frame is introduced, surrounded by the previous iteration. This self-similar geometry further extends the current paths and increases the edge density, thereby strengthening field confinement and improving the impedance matching. The fractal nature of the structure enables multiresonant behavior or an enhanced bandwidth, depending on the design parameters. The simulated transmission coefficient for this case is $S_{21} = -10.306$ dB at Freq. $= 4$ GHz. Finally, for more details on the geometric dimensions, see Fig. 2(f). The final optimized dimensions were obtained as follows: $a = 7$ mm, $b = 20$ mm, $c = 11$ mm, $d = 2$ mm, $e = 4$ mm, $f = 6$ mm, and $g = 18$ mm. These improved values contributed to enhancing the overall characteristics of the sensor at the target operating frequency.

In conclusion, the transition from the traditional patch to the higher-order fractal design demonstrates the effectiveness of fractal engineering in a microstrip sensor for impedance matching, compactness, and a stronger electric field. The comparison of S_{21} values among the five designs emphasizes the effect of fractal iteration on the resonance characteristics of the resonator, thus supporting the use of fractal designs in wireless and sensing technologies.

From an electromagnetic perspective, the cross-shaped microstrip structure operates as a resonator, where the effective electrical length of the arms determines the resonant frequency. At resonance, the strong electric field density (v/m) is concentrated around the edges, as shown in Fig. 4(a), making the structure highly sensitive to perturbations in the surrounding medium. When a material under test (MUT), such as edible oil, is placed in proximity to or directly on the sensing region, changes in its dielectric properties, particularly the permittivity and loss tangent, modify the effective capacitance and inductance of the resonator. As a result, measurable shifts in the resonance frequency and variations in the transmission coefficient magnitude ($|S_{21}|$) were observed. Fig. 4(b) illustrates two quartz tubes with an inner diameter of 1 mm, placed in the region where the maximum electric fields were constructed. We utilize two tubes for loading the MUT, and the two sides of the resonator response are perturbed symmetrically.

The simulation was carried out by adjusting the transmission line position to have a 90° position to form an L-shaped arrangement. The simulation outcomes showed the presence of distortion in the S_{21} curve, wherein the highest transmission peak was attained at -29.66 dB for a resonant frequency of 3.92 GHz, as shown in Fig. 5(a). In addition, Fig. 5(b) shows the distribution of electric field density, which has been significantly reduced in comparison to the proposed model (see Fig. 4(a)). Reduced electric field confinement decreases the MUT-electromagnetic field interaction, which limits sensor sensitivity and measurement accuracy.

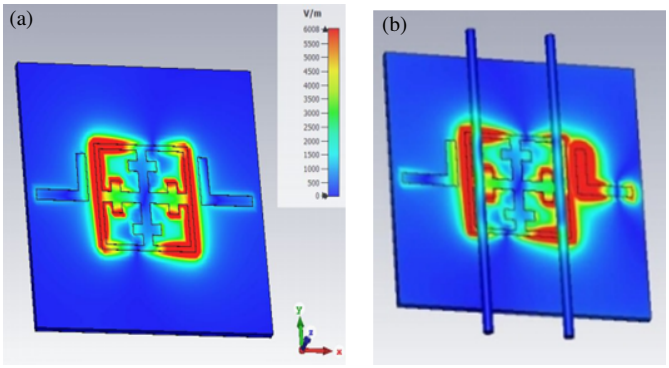

FIGURE 4. Numerical prediction for surface electric field distribution (v/m) around slots of the resonator at 4 GHz (a) without tubes. (b) the interaction of the maximum electric field with two quartz tubes.

The proposed sensor was fabricated by using a chemical etching technique after selecting the final dimensions and evaluating them numerically using the CST program, as shown in Fig. 6(a). In real world sensing, the sensor is usually characterized using a vector network analyzer (VNA-KC901V), where the transmission response is measured within a certain frequency range (see Fig. 6(b)).

3. SENSOR TESTED

To verify the correctness of the results of the fabrication process and their matching with the results of the simulation process, this section assesses the performance of the sensor in detecting the liquids filled inside the quartz tubes. The electrical permittivity ($\varepsilon_r = \varepsilon' + j\varepsilon''$) was calculated, and the results were compared with the theoretical values.

The simulated and measured results, shown in Figs. 7(a) and 7(b), respectively, illustrate the insertion loss (S_{21}) vs. frequency response from 2 to 6 GHz using empty tubes (air), and when they were filled with common solvents (DI-water and ethanol), all these results were measured at room temperature, 25°C. The operation of the sensor is dependent upon the placement of the samples in relation to the electric field interaction area. Given that the operation of the proposed sensor is dependent upon the perturbation of the electromagnetic field, different placements of samples may interfere with the resonance frequency and transmission responses. For consistency purposes in making measurements, all experiments were carried out with the sensors positioned in the same spot within a laboratory environment at room temperature of 25°C. Moreover, the position of the sensing area was selected using the maximum value of the electric field intensity from simulations, as depicted in Fig. 4(b).

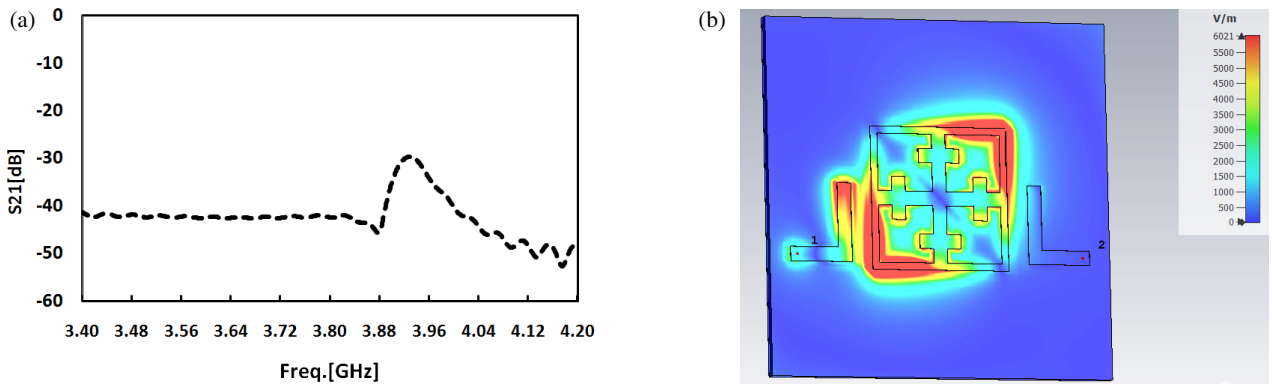

FIGURE 5. (a) Numerical S_{21} parameter of the resonator after changing the position of the coupling transmission lines. (b) Surface electric field distribution (v/m) @3.92 GHz.

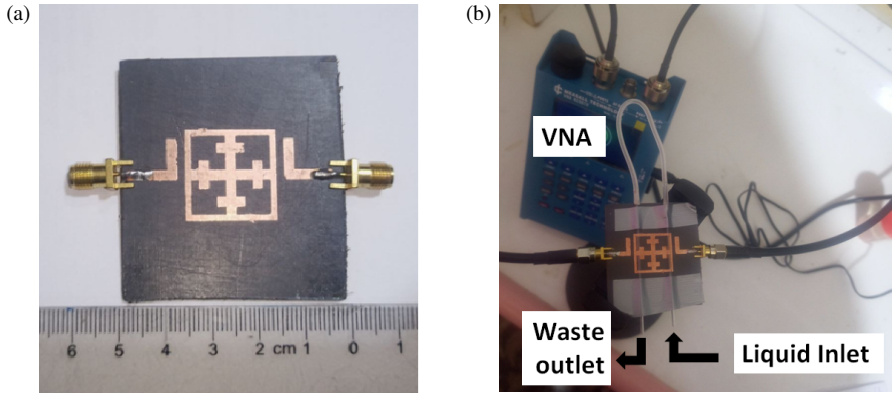

FIGURE 6. (a) The fabricated sensor prototype and (b) calibration and experimental setup for the S_{21} parameter measurement protocol with the VNA.

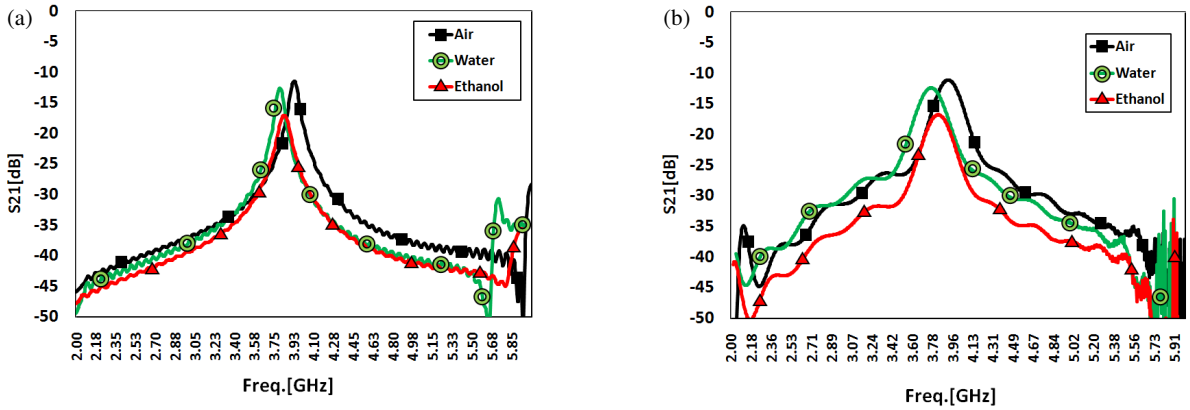

FIGURE 7. S_{21} profile for effect dielectric liquids. (a) Simulation results, (b) experimental results.

Table 1 shows the extracted data from Fig. 8. The data include the resonant frequency (Freq.) and insertion loss (S_{21}), which have been used to calculate the complex permittivity (ε_r) by applying the Debye Model (theoretical model) [21, 22]. The theoretical data of the Debye Model are also presented in Table 2.

To assess the accuracy of the sensor, the measured results were compared with the simulation ones, where a small difference between them indicated a low error. This error was calculated as the difference between the simulated and measured resonant frequencies relative to the free-loader resonant frequency [16, 23]. However, due to various reasons, there is a minimal variation between them. Some of these reasons may include tolerance in manufacture, mistakes in the relative permittivity of quartz tubes, and problems in calibrating the vector network analyzer employed in the experiment. Moreover, the location of the tubes with respect to the region of interaction

TABLE 1. Simulated and measured values of resonance characterize when tubes loaded with MUT.

	Resonant Characterize	Air	Water	Ethanol
Simulated	Freq. (GHz)	3.925	3.7625	3.827
	S_{21} (dB)	−11.45	−12.59	−17.02
Measured	Freq. (GHz)	3.919	3.7615	3.822
	S_{21} (dB)	−11.06	−12.35	−16.74
Error %		0.15	0.03	0.13

with the electric field may affect the results. The error values for the proposed sensor are presented in Table 1.

The measurement and simulation results were identical. Moreover, the sensor exhibited remarkable sensitivities of 0.86% and 3.56% and an average error of 0.1%, with frequency shifts of 163 and 103 MHz for water and ethanol detection, respectively.

4. RESULTS AND DISCUSSION

As shown in Fig. 8, four edible oil samples, including coconut oil, olive oil, sunflower oil, and sesame oil, are used in this study for sensing validation, characteristics, especially due to a similar yellowish colouration, as well as similar odour profiles. Due to these similarities, reliable discrimination based on human perception is difficult and subjective.

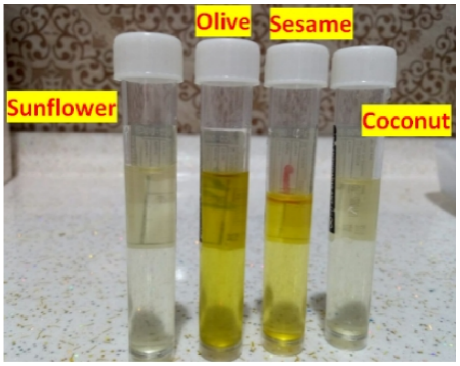

FIGURE 8. Coconut oil, olive oil, sunflower oil, and sesame oil samples as MUT.

Thus, in the context of the present study, resonant microwave sensor-based detection was used as an alternative objective method. The resonant properties of microwave sensors allow for the sensitive characterization of the dielectric properties of vegetable oils, which can be differentiated based on their types, but cannot be reliably differentiated based on human perception.

The Vector Network Analyzer (VNA) was tuned to plot the sensor loss curve (S_{21}) in the range of 3.6–4.1 GHz when the two quartz tubes were loaded with the edible oils, as shown in Fig. 9. New tubes were used for each oil sample because no air bubbles were present between the oil fluids. The position,

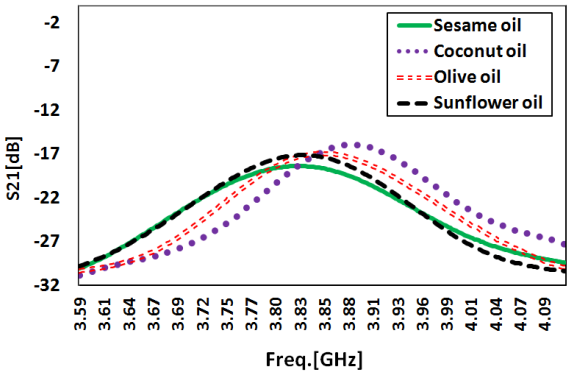

FIGURE 9. Measured S_{21} of the sensor when the tubes were loaded with several edible oils.

shape, and intensity of these peaks were quite different for the various oils in relation to the complex permittivity values.

For instance, sesame oil showed a prominent maximum peak at approximately −18.32 dB at 3.838 GHz. However, at a frequency of 3.847 GHz, olive oil exhibits a peak near −16.84 dB, while sunflower oil and coconut oil demonstrate S_{21} peaks at around −17.09 dB and −15.84 dB at frequencies of 3.843 GHz and 3.873 GHz, respectively. Introducing small amounts of dielectric materials near the electric peak regions distorts the resonator response, allowing the composite permittivity ($\varepsilon_r = \varepsilon' + j\varepsilon''$) of the samples to be estimated from the resonant frequency shift and the change in the quality factor. For lossless samples, the dielectric constant (ε') can be directly deduced from the change in resonant frequency.

Because Debye model parameters for vegetable oils are unavailable in the scientific literature at microwave frequencies, this study employs numerical simulation to construct a numerical model capable of calculating the complex permittivity of these oils based on the resonant frequency extracted from the proposed sensor.

In the first stage, a virtual liquid material was defined in the simulation program with a real dielectric permittivity ranging from $\varepsilon' = 1$ to $\varepsilon' = 80$ and a loss coefficient (the imaginary part of the permittivity) ranging from $\varepsilon'' = 0.01$ to $\varepsilon'' = 15$. This is intended to cover the expected range of properties of various liquids, including vegetable oils. Subsequently, a series of simulations was performed with varying complex permittivity values, and the corresponding resonant frequency for each case was extracted based on the position of the lower values of the transition coefficient curve $|S_{21}|$.

Figure 10 illustrates the relationship between the complex permittivity ($\varepsilon' + j\varepsilon''$) and the resonant frequency at the laboratory temperature. In the next step, to construct an accurate mathematical model, curve fitting was performed on the data extracted from Fig. 10(a). A mathematical equation representing the relationship between the real part of the permittivity (ε') and the resonant frequency was derived, as shown in Equation (1), which exhibited a high determination factor of $R^2 = 0.999$, indicating the accuracy of the proposed model.

Based on the data shown in Fig. 10(b), a similar mathematical model was constructed to extract the loss coefficient (the imaginary part of the permittivity — ε'') as a function of the resonant

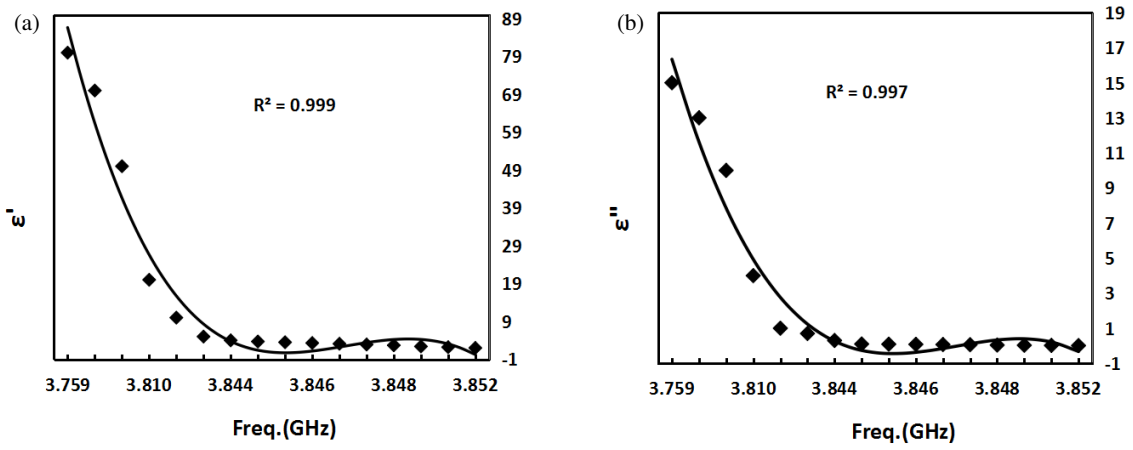

FIGURE 10. Numerical spectrum of permittivity (ε' & ε'') as a function of frequency with a fitting curve line at a temperature selection of 25°C.

TABLE 2. Comparison of the theoretical and numerical models to compute the complex permittivity of the MUT.

MUT	Freq. (GHz)	Theoretical model		Numerical model		Sensitivity (%)	
		ε'	ε''	ε'	ε''	$f_{0(\text{air})}$	$f_{0(\text{water})}$
DI-water	3.762	75.6	13.7	75.64	14.28	0.86	0
Ethanol	3.822	12.4	4.82	12.35	4.18	3.56	0.37
Coconut oil	3.873	n/a	n/a	3.72	0.31	7.49	0.6
Olive oil	3.847	n/a	n/a	3.00	0.07	15.2	0.44
Sunflower oil	3.843	n/a	n/a	3.84	0.30	11.3	0.42
Sesame oil	3.838	n/a	n/a	5.24	0.64	8.05	0.41

frequency. This relationship is represented by Equation (2). This model also achieved high accuracy, with a determination factor of $R^2 = 0.997$, confirming the model's reliability in estimating the complex electrical properties of vegetable oils based on resonant measurements. The polynomial regression analysis revealed a high degree of agreement between frequency and complex permittivity, with a coefficient of determination (R^2) ranging between 0.997 and 0.999.

$$\varepsilon' = 117080.64 - 60689.9 \times \text{Freq.} + 7864.93 \times (\text{Freq.})^2 \quad (1)$$

$$\varepsilon'' = 20244.36 - 10474.37 \times \text{Freq.} + 1354.82 \times (\text{Freq.})^2 \quad (2)$$

The resonant characteristics of the sensor recorded in Table 2 were extracted from these results, which were used to calculate the complex permittivity (ε_r) using the Debye Model (theoretical model), and the numerical model is presented in Table 2 for comparison.

To validate the proposed mathematical model, the same methodology was applied to reference liquids with known electrical properties, namely water and methanol, for which Debye model parameters are available in the literature. The complex permittivity values extracted using the proposed numerical model were compared with those calculated using the Debye model at the same resonant frequency.

The results showed a high degree of convergence between the values extracted from the proposed mathematical model and those calculated using the Debye model for both water and methanol, with only minor differences within the practically acceptable limits. This agreement confirms the ability of the proposed model to accurately represent the electromagnetic behavior of liquids, thus enhancing its reliability in estimating the complex permittivity of vegetable oils, for which reliable Debye parameters are not available.

Therefore, the proposed mathematical model can be adopted as an effective tool for calculating the complex permittivity of liquids based on the resonant frequency, without requiring prior knowledge of the Debye model parameters. This makes it suitable for practical applications in non-contact microwave sensing systems.

The sensor exhibited maximum sensitivities of 15.23% and 11.32% for olive oil and sunflower oil, respectively, with respect to the empty tube (air) results as reference sample, as listed in Table 2. Equation (3) was used to calculate the relative sensitivity of the proposed sensor [4, 5, 13], where f_0 and ε'_0 denote the reference sample, and f_1 and ε'_1 denote the MUT.

$$\text{Sensitivity}\,(\%) = \left| \frac{f_0 - f_1}{(\varepsilon'_0 - \varepsilon'_1) f_0} \right| \times 100 \quad (3)$$

Therefore, the adulteration of vegetable oils by increasing the proportion of added DI water can be detected by the sensor through changes in its resonant properties, such as a change in the resonant frequency. A significant change was observed in the frequency shift (f_0-f_1), which represents the sensor efficiency, where f_0 (3.762 GHz) and ε'_0 (75.64) denote the DI water, and f_1 and ε'_1 refer to edible oil results. The sensor shows

TABLE 3. Comparison with other related works.

Ref.	Freq. (GHz)	Max. sensitivity %	Application	Resonant type	Dimensions (mm^2)
[1]	8–9	0.5	Milk and dairy product	Metamaterial-based sensor	22.86×10.15
[4]	8–12	n/a	Edible oil detection	SRR shaped metamaterial	22.86×10.16
[5]	3.21	11.04	Characterization of edible oils	CSRR-based antenna	20×15
[6]	2.523	2.42	Edible oils and various liquid materials	(CDSRR)-based antenna	60×60
[7]	2.2 & 5.2	10.62	Various oil samples, toluene, and ethanol	TSSRR-based antenna	9×31.32
[8]	2.4	1.52	Common liquid samples (methanol and ethanol)	DS-CSRR-based sensor	50×60
[9]	2.508	0.69	Various liquid materials	CDSRR-based antenna	60×60
[10]	2.5	7.321	Common liquid (ethanol, methanol, DI water)	TR-CSRR-based sensor	25×20
[11]	2.4	0.015	Na_2SO_3 concentrations	Star-fractal antenna	45×55
[12]	3.12	6.39–6.54	Detection of carbamate	CLRR-based sensor	86×75
[13]	7.32	6.35	Engine oils and alcohols	Metamaterial (CSRRs)-based microwave sensor	25×15
[14]	5.53	1.7	Engine oil	GHz sensor	30×5
[16]	2.24	1.43–0.95	Solid/liquid	Sensor based on a band-stop filter	7×14
T.W	**3.8**	**15.23**	**Edible oil**	**Fractal sensor-based Māra cross-shaped**	**50×50**

TABLE 4. Comparison of dielectric properties of edible oil versus state-of-the-art microwave sensors.

Ref.	Band	Edible oil	Dielectric constant	Error 100%
[4]	X	olive	2.54	n/a
		sunflower	2.92	
		coconut	2.16	
[5]	S	olive	3.1	0.83–5.42
[6]	S	olive	3.1	0–0.55
[7]	L	olive	3.1	0.2–0.5
[24]	X	olive	2.54	n/a
[25]	X	olive	1.79	n/a
[26]	UHF-S	olive	> 2.6	n/a
T.W	**S**	**olive**	**3**	**0.03–0.15**
		sunflower	**3.84**	
		coconut	**3.72**	
		sesame	**5.24**	

an excellent sensitivity ranging from 0.4% to 0.6% with a frequency shift between 76.5 and 111.5 MHz. The recorded data in Table 2 show the normalized sensitivities of 0.44% and 0.42% with frequency shifts of 85.5 and 81.5 MHz for olive oil and sunflower oil, respectively. Coconut oil shows a maximum accuracy with 0.6% with a higher-frequency shift of 111.5 MHz, whereas sesame oil shows a minimum frequency change of 76.5 MHz with a sensitivity of 0.41%.

A practical experiment was conducted to detect oil adulteration, using a coconut oil sample as the reference sample, to which 25% DI water was added. The resonant characteristics of the MUT (coconut oil +25% water) were recorded as follows: f_1 of 3.862 GHz, ε'_1 of 0.37, and the sensitivity of the sensor was 1.27%. Moreover, the experimental results confirm that the proposed sensor achieves enhanced sensitivity compared to that reported in the literature, as illustrated in Table 3.

As per the findings shown in Table 3, it has been noticed that the relative sensitivity of the fractal sensor proposed is higher than the ones described in the literature. Concerning the geometric dimensions of the proposed sensor, some of the sensors found in literature were smaller than the proposed one, while others were larger.

To strengthen the overall evaluation of the proposed study, a comparison of the measured dielectric constant ranges of edible oils is added to Table 4. It also demonstrates that this work has accomplished a lower level of error than that in [5–7].

5. CONCLUSION

This study presents the development and application of a portable and cost-effective microwave sensor for detecting edible oils. The proposed sensor is highly sensitive and accurate for measuring the dielectric properties of the MUT.

The symmetric cross design has several advantages over conventional linear or ring resonators. The design improves the confinement of the field at multiple arms, thus increasing the interaction region between the electromagnetic field and MUT, which is essential for enhancing the sensitivity and resolution. The cross-shaped microstrip sensor has many applications in chemical and biological sensing and nondestructive testing, especially in the microwave and millimeter wave frequency ranges.

REFERENCES

[1] Abdulkarim, Y. I., M. Bakır, I. Yaşar, H. Ulutaş, M. Karaaslan, F. O. Alkurt, C. Sabah, and J. Dong, "Highly sensitive metamaterial-based microwave sensor for the application of milk and dairy products," *Applied Optics*, Vol. 61, No. 8, 1972–1981, 2022.

[2] Priyanka, S. Bansal, and P. Kaur, "CSRR based microstrip patch antenna sensor for the analysis of water and milk quality," *Indian Journal of Engineering and Materials Sciences (IJEMS)*, Vol. 32, No. 1, 122–130, 2025.

[3] Al-Mudhafar, A. A., R. A. Malallah, S. J. Ghazi, and A. A. Al-Mudhafar, "A multiband microwave sensor designed to sense the shelf life of raw fresh milk," *IEEE Sensors Journal*, Vol. 24, No. 21, 35 538–35 546, 2024.

[4] Islam, M. R., M. T. Islam, A. Hoque, M. S. Soliman, B. Bais, N. M. Sahar, and S. H. A. Almalki, "Tri-circle split ring resonator shaped metamaterial with mathematical modeling for oil concentration sensing," *IEEE Access*, Vol. 9, 161 087–161 102, 2021.

[5] Dhar, S., P. Paul, S. Mandal, and G. Sen, "Preparation design and implementation of a portable microwave sensor for characterization of edible oils," *IEEE Sensors Letters*, Vol. 8, No. 12, 1–4, 2024.

[6] Mandal, S., S. Bal, S. Banerjee, and G. Sen, "3D-printed microstrip patch antenna sensor utilizing complementary dual split-ring resonator for detection of liquid samples," *Frequenz*, Vol. 80, No. 1–2, 39–45, 2026.

[7] Karak, S., S. Mandal, A. Ghosh, and G. Sen, "A compact dual band antenna sensor for multiband sensing application," *IEEE Sensors Letters*, Vol. 10, No. 3, 1–4, 2026.

[8] Beria, Y., G. S. Das, A. Buragohain, and B. B. Chamuah, "Highly sensitive miniaturized octagonal DS-CSRR sensor for permittivity measurement of liquid samples," *IEEE Transactions on Instrumentation and Measurement*, Vol. 72, 1–9, 2023.

[9] Sen, G., S. Mandal, and M. Gangopadhyay, "Compact CDSRR-based antenna for sensing applications," in *2024 IEEE International Conference on Electronics, Computing and Communication Technologies (CONECCT)*, 1–5, Bangalore, India, 2024.

[10] Al-Gburi, A. J. A., Z. Zakaria, N. A. Rahman, A. A. Althuwayb, I. M. Ibrahim, T. Saeidi, Z. A. Dayo, and S. Ahmad, "A miniaturized and highly sensitive microwave sensor based on CSRR for characterization of liquid materials," *Materials*, Vol. 16, No. 9, 3416, 2023.

[11] Al-Mudhafar, A. A. and R. A. Malallah, "New star-fractal antenna devised as wireless sensor of the permittivity characterization measurement of Na_2SO_3 solutions," *Microsystem Technologies*, Vol. 28, No. 9, 2149–2157, 2022.

[12] Wongsa, F., S. Phunklang, A. Yueanket, S. Kornsing, N. Santalunai, P. Mesawad, S. Santalunai, S. Narakaew, and P. Krachodnok, "Quantitative detection of carbamate pesticide residues in vegetables using a microwave ring resonator sensor," *Applied Sciences*, Vol. 15, No. 21, 11775, 2025.

[13] Kumar, K. S. and M. G. Madhan, "A novel metamaterial-based microwave sensor design for the characterization of lubricating engine oils and alcohols," *Journal of Optoelectronics and Advanced Materials*, Vol. 27, No. 9–10, 427–438, 2025.

[14] Arumugam, J., N. R. Edhayaraj, S. Shanmugavadivelu, and V. Sathyanarayanan, "Design of microwave electromagnetic sensor for liquid characterization," *Journal of High-Frequency Communication Technologies*, Vol. 1, No. 3, 73–83, 2023.

[15] Al-Mudhafar, A. A., A. A. Abduljabar, and H. J. Albattat, "Breakdown voltage measurement of high voltage transformers oils using an active microwave resonator sensor," *International Journal of Electronics and Communication Engineering*, Vol. 17, No. 3, 84–88, 2023.

[16] Rasoulzadeh, A., C. Ghobadi, J. Nourinia, and P. Mohammadi, "A highly sensitive and compact size microstrip sensor for characterization of solid and liquid material with broad range permittivity," *IEEE Access*, Vol. 12, 87 864–87 872, 2024.

[17] Al-Mudhafar, A. A., "Circular patch 1×2 active antenna array for 5G applications," *International Journal of Communication Systems*, Vol. 39, No. 4, e70425, 2026.

[18] Navaei, M., P. Rezaei, and S. Kiani, "A symmetric bar chart-shape microwave sensor with high Q-factor for permittivity determination of fluidics," *International Journal of Microwave and Wireless Technologies*, Vol. 15, No. 8, 1334–1342, 2023.

[19] Navaei, M., P. Rezaei, and S. Kiani, "Measurement of low-loss aqueous solutions permittivity with high detection accuracy by a contact and free-label resonance microwave sensor," *International Journal of Communication Systems*, Vol. 36, No. 5, e5417, 2023.

[20] Karami, M., P. Rezaei, S. Kiani, and R. A. Sadeghzadeh, "Modified planar sensor for measuring dielectric constant of liquid materials," *Electronics Letters*, Vol. 53, No. 19, 1300–1302, 2017.

[21] Debye, P., *Polar Molecules*, Chemical Catalog Co., New York, NY, USA, 1929.

[22] Buckley, F. and A. A. Maryott, *Tables of Dielectric Dispersion Data for Pure Liquids and Dilute Solutions*, National Bureau of Standards Circular, Nov. 1958.

[23] Kiani, S., P. Rezaei, and M. Navaei, "Dual-sensing and dual-frequency microwave SRR sensor for liquid samples permittivity detection," *Measurement*, Vol. 160, 107805, Aug. 2020.

[24] Bakır, M., S. Dalgaç, M. Karaaslan, F. Karadağ, O. Akgol, E. Unal, T. Depçi, and C. Sabah, "A comprehensive study on fuel adulteration sensing by using triple ring resonator type metamaterial," *Journal of the Electrochemical Society*, Vol. 166, No. 12, B1044–B1052, 2019.

[25] Viskadourakis, Z., A. Theodosi, K. Katsara, M. Sevastaki, G. Fanourakis, O. Tsilipakos, V. M. Papadakis, and G. Kenanakis, "Engraved split-ring resonators as potential microwave sensors for olive oil quality control," *ACS Applied Electronic Materials*, Vol. 6, No. 5, 3846–3856, May 2024.

[26] Chen, C. and S.-Y. Wang, "A high-sensitivity microwave patch sensor for olive oil adulteration detection," *Progress In Electromagnetics Research C*, Vol. 167, 155–164, 2026.